ADVANCES IN ATMOSPHERIC SCIENCES, VOL. 28, NO. 6, 2011, 1345–1356

Relationship Between East Asian Winter Monsoon and Summer Monsoon

YAN Hongming*[1] (晏红明), YANG Hui[2] (杨 辉), YUAN Yuan[3] (袁 媛), and LI Chongyin[2,4] (李崇银)

[1] *Yunnan Climate Center, Kunming* 650034

[2] *State Key Laboratory of Numerical Modeling for Atmospheric and Geophysical Fluid Dynamics, Institute of Atmospheric Physics, Chinese Academy of Sciences, Beijing* 100029

[3] *National Climate Center, Beijing* 100081

[4] *School of Meteorology, PLA University of Science and Technology, Nanjing* 211101

(Received 16 October 2010; revised 10 March 2011)

ABSTRACT

Using National Centers for Environmental Prediction/National Centre for Atmospheric Research (NCEP/NCAR) reanalysis data and monthly Hadley Center sea surface temperature (SST) data, and selecting a representative East Asian winter monsoon (EAWM) index, this study investigated the relationship between EAWM and East Asian summer monsoon (EASM) using statistical analyses and numerical simulations. Some possible mechanisms regarding this relationship were also explored. Results indicate a close relationship between EAWM and EASM: a strong EAWM led to a strong EASM in the following summer, and a weak EAWM led to a weak EASM in the following summer. Anomalous EAWM has persistent impacts on the variation of SST in the tropical Indian Ocean and the South China Sea, and on the equatorial atmospheric thermal anomalies at both lower and upper levels. Through these impacts, the EAWM influences the land–sea thermal contrast in summer and the low-level atmospheric divergence and convergence over the Indo-Pacific region. It further affects the meridional monsoon circulation and other features of the EASM. Numerical simulations support the results of diagnostic analysis. The study provides useful information for predicting the EASM by analyzing the variations of preceding EAWM and tropical SST.

Key words: East Asian winter monsoon, East Asian summer monsoon, interannual variation, interaction, possible mechanism

Citation: Yan, H. M., H. Yang, Y. Yuan, and C. Y. Li, 2011: Relationship between East Asian winter Monsoon and summer monsoon. *Adv. Atmos. Sci.,* **28**(6), 1345–1356, doi: 10.1007/s00376-011-0014-y.

1. Introduction

The Asian monsoon plays a key role in general atmospheric circulation and climate variations. The East Asian winter monsoon (EAWM), an important component of the Asian monsoon system, is the strongest winter monsoon globally. Its variation may not only control the local weather and climate in East Asia but may also exert a strong impact on the extratropical and tropical planetary-scale circulations (Chang and Lau, 1982). The EAWM also influences the convection over and the sea-surface temperature (SST) near the maritime Asian continent (Zhang et al., 1997). This influence can lead to anomalous summer circulation accompanied by drought or floods in many areas (Chen et al., 2000). Therefore, further studies on the variations of EAWM and its effects on winter and summer climates are important for understanding climate variations and for improving the prediction of such variations.

The most representative factors of EAWM and EASM activities are the following: winter surface temperature over East Asia and the East Asian trough (EAT), summer precipitation over eastern China, and meridional and zonal winds in the lower and upper troposphere over East Asia in both winter and summer (Chen et al., 1991; Ding, 1994; Jhun and Lee., 2004; Gao, 2007; Li and Yang, 2010). Therefore, many stud-

*Corresponding author: YAN Hongming, y-hm@netease.com

ies have investigated the variability in these factors to reveal the anomalous features of EAWM and its influence on the summer climate over East Asia. Some studies found that the drought and floods over the Yangtze River and the Huaihe River valleys in summer are closely related to the variation of the EAT in winter, suggesting that less summer precipitation over the Yangtze River and the Huaihe River valleys occurs after a strong EAWM, and vice versa (Sun and Sun, 1995; Chen and Sun, 1999). By defining strong and weak EAWM years based on meridional winds at 10-m height, Chen et al. (2000) analyzed anomalous stream fields at 850 hPa in summer, and they found the variation of the subtropical western Pacific high (SWPH) to be obviously different during strong and weak EAWM years. The SWPH tends to be more northward in the summer following strong EAWM and more southward in the summer following weak EAWM. The close relationship between the SWPH and the strength of the EASM has been emphasized in observational analyses by Guo (1985), who suggested that the SWPH shifted to the north in strong EASM years and to the south in weak EASM years. These studies, to a large extent, imply some possible linkages between EAWM and EASM.

For climate prediction, the early variations of atmospheric circulation, SST, and snow cover are key factors. Like SWPH, an important circulation system for China's climate, is closely related to both EAWM and EASM. Therefore, the studies on the interactions and interrelationships between winter and summer atmospheric circulation are important to improving the accuracy of climate prediction.

Meteorological data used in this study were derived from the National Centers for Environmental Prediction/National Centre for Atmospheric Research (NCEP/NCAR) reanalysis (Kistler et al., 2001), including monthly three-dimensional winds on 12 standard pressure levels, with a horizontal resolution of $2.5^\circ \times 2.5^\circ$ grid over a 57-year period (1948–2004). Monthly SST data were mainly obtained from the Hadley Center sea ice and SST dataset (HadISST), with $1^\circ \times 1^\circ$ resolution over a 57-year period (1948–2004; Rayner et al., 2003). Utilizing correlation analyses, composite analyses, and a general circulation model (GCM), the relationship between EASM and EAWM, as well as the possible mechanisms of their linkage were investigated, and the results of this study are presented here.

2. Relationship between EAWM and EASM

Many factors can represent EAWM and EASM activities, such as surface temperature, sea level pressure (SLP), EAT, meridional winds in the lower troposphere, zonal winds in the upper troposphere, summer precipitation in East Asia, and a geopotential height of 500 hPa (Guo, 1983; Shi, 1996; Cui and Sun, 1999; Wu and Huang, 1999; Chen et al., 2000; Yan et al., 2003; Wang and Chen., 2010). Among these factors, summer precipitation exhibits regionally different characteristics, while some other factors, such as meridional wind, surface temperature, and SLP in winter, are relatively stable, making them the most popular indices used in EAWM or EASM research. Based on surface temperature, SLP, geopotential height at 500 hPa, and meridional wind factors, this section presents the results of our study of the relationship between EAWM and EASM using composite and correlation analyses.

Considering the influence of EAWM on middle- and low-latitude climate over East Asia, and based on the analyses of various factors that can represent, to some extent, the EAWM variation, Yan et al. (2009) defined a composite EAWM index using surface temperature, SLP, geopotential height at 500 hPa from December to February (December-January-February, DJF), namely

$$I_{\mathrm{EAWM}} = [\frac{I_{\mathrm{H500}}}{s_{\mathrm{H500}}} + \frac{I_{\mathrm{SLP}}}{s_{\mathrm{SLP}}} + \frac{I_{\mathrm{AIR995}}}{\mathrm{s}_{\mathrm{AIR995}}}]/3\,.$$

In this equation, I_{H500} denotes the regionally averaged potential height anomalies at 500 hPa over the area (25°–40°N, 115°–140°E), $I_{\mathrm{H500}} = \overline{H}_{500} - \overline{\overline{H}}_{500}$; $I_{\mathrm{SLP}} = (\overline{P}_{\mathrm{SL}}|_{20}^{50} - \overline{\overline{P}}_{\mathrm{SL}}|_{20}^{50})_{110} - (\overline{P}_{\mathrm{SL}}|_{20}^{50} - \overline{\overline{P}}_{\mathrm{SL}}|_{20}^{50})_{160}$ mainly denotes the different SLP between 110°E (land) and 160°E (sea). $\overline{P}_{\mathrm{SL}}|_{20}^{50}$ is the mean SLP from 20°N to 50°N respectively in 110°E and 160°E, and $\overline{\overline{P}}_{\mathrm{SL}}|_{20}^{50}$ is the multi-annual mean of corresponding $\overline{P}_{\mathrm{SL}}|_{20}^{50}$; I_{AIR995} denotes the surface temperature anomalies over East Asia (20°–40°N, 110°–135°E), $I_{\mathrm{AIR995}} = \overline{T}_{\mathrm{AIR995}} - \overline{\overline{T}}_{\mathrm{AIR995}}$. Here $S_{\mathrm{H500}}, S_{\mathrm{SLP}}$, and S_{AIR995} are the corresponding standard deviations. "–" denotes regional average and "=" denotes multi-annual mean of regional average value. The index I_{EAWM} reflected well the circulation feature of EAWM. According to the variation of I_{EAWM}, we selected strong EAWM years (1953, 1955, 1956, 1962, 1963, 1968, 1974, 1977, 1981, 1984, 1986) and weak EAWM years (1973, 1979, 1989, 1990, 1998) for study. Here 1953 indicates the 1952/1953 winter (December 1952, January 1953, and February 1953), etc. Comparing the above strong and weak EAWM years with other research (Chen et al., 1999; Chen et al., 2000; Jhun et al., 2004), most strong and weak years are the same, especially 1973, 1977, 1979, 1984, and 1986. Because the low-level winds over East Asia in winter (DJF) and summer (JJA) can reflect EAWM and EASM activities, the composite 850-hPa wind anomalies in winter and summer during strong or weak EAWM years are presented in Figs. 1a–d. Clearly, northeasterly winds during strong EAWM cases were enhanced along the

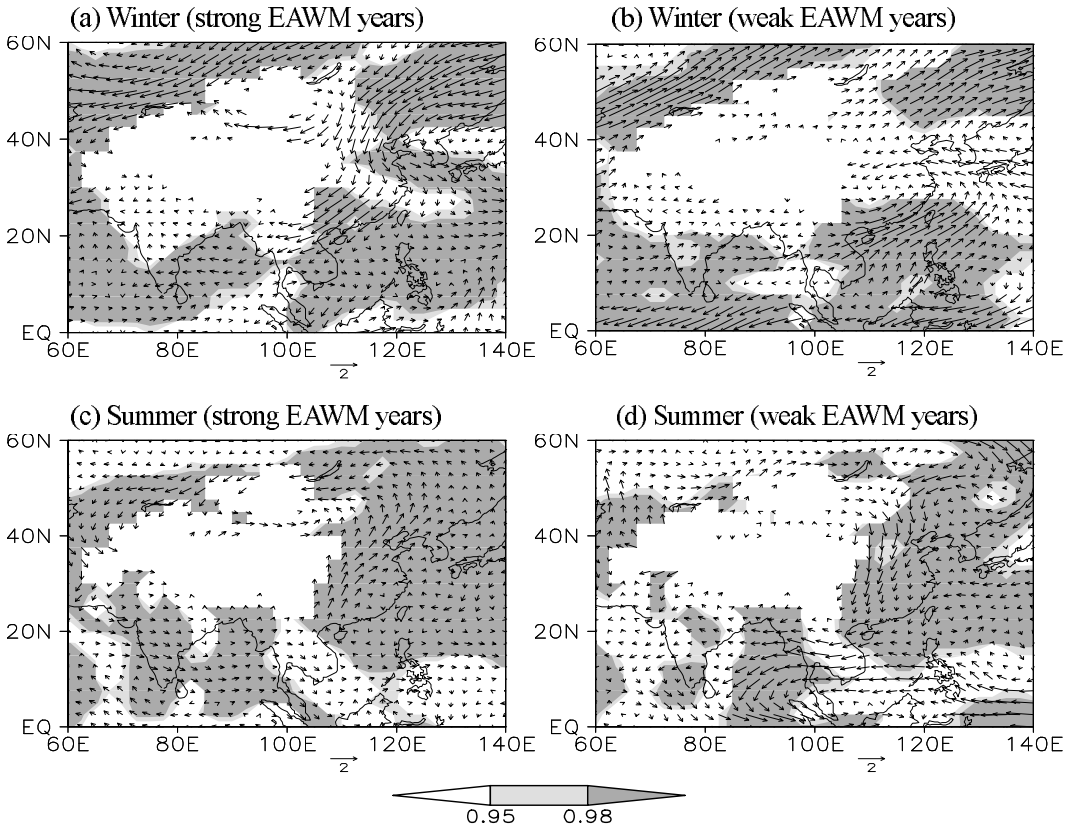

Fig. 1. Composite 850-hPa wind anomalies respectively in (a, b) winter and (c, d) summer in (a, c) strong and (b, d) weak EAWM years. Shading indicates the composite wind exceeding the 95% confidence level of the student t-test.

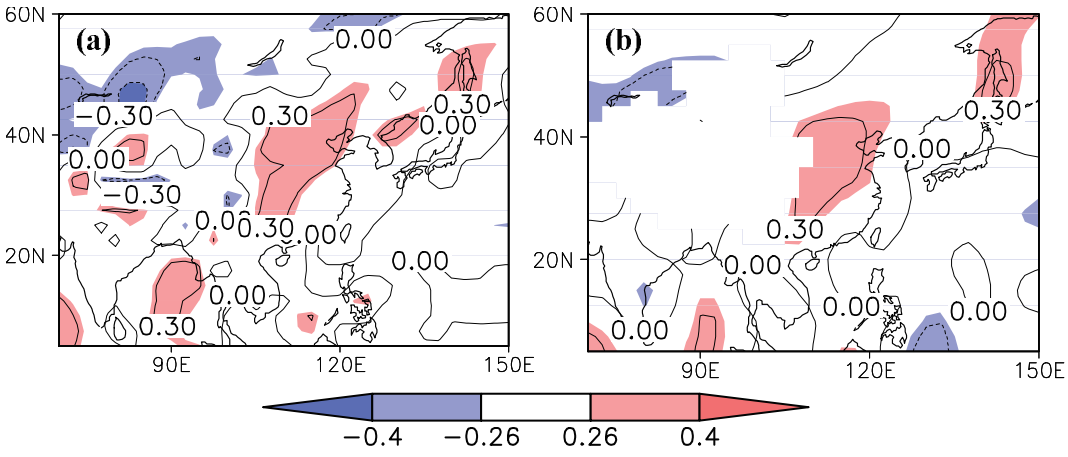

Fig. 2. Correlation coefficients between the EAWM index I_{EAWM} and the meridional wind at (a) surface and (b) 850 hPa in JJA from 1949 to 2004. Shading indicates the correlation coefficient exceeding 95% confidence level.

East Asian coast and extended southward toward the equator in winter (Fig. 1a), while anomalous southwesterly winds occurred over East Asia in the subsequent summer, enhancing the EASM (Fig. 1c). On the contrary, during weak EAWM years, anomalous southwesterly winds occurred along the East Asian coast in winter (Fig. 1b) and anomalous northerly winds occurred over the East Asian region in the subsequent summer (Fig. 1d). The anomalous winds over East Asia exceeded the 95% confidence level of student t-test. To some extent, these distributions of anomalous wind show that strong EAWM is advantageous for the occurrence of strong EASM in following summer and that weak EAWM is advantageous for the occurrence of weak EASM in following summer.

Apart from this analysis, we calculated the correlation between the $I_{\rm EAWM}$ (Yan et al., 2009) and the meridional winds, respectively, at surface level (Fig. 2a) and at 850 hPa in JJA (Fig. 2b). Higher positive correlations exceeding the 95% confidence level were located over East Asia, and its central value was >0.4. The correlation field also displayed an in-phase variation between EAWM and EASM: a strong EASM occurred in summer following a previous strong EAWM in winter and a weak EASM in summer occurred following a previous weak EAWM in winter. The distributions of correlation coefficients in Figs. 2a and 2b are very similar, but the area of higher positive correlation exceeding the 95% confidence level over East Asia in Fig. 2b is larger than that in Fig. 2a, indicating that the correlation between EAWM and meridional winds at 850 hPa is more obvious.

To further substantiate the above claim, we analyzed the previous circulation characteristics based on the $I_{\rm EAWM}$, defined as the seasonally (JJA) averaged value at 850 hPa within the East Asian monsoon domain (10°–40°N, 110°–140°E; Li and Zeng, 2002, 2003, 2005). Figure 3 depicts the composite wind anomalies at 850 hPa in preceding winter of strong EASM years (1949, 1951, 1961, 1962, 1963, 1973, 1985, 1998) and weak EASM years (1957, 1981, 1984, 1989, 1996, 1997, 1999, 2004, 2009). Shaded areas indicate significantly anomalous winds at the 95% confidence level. Clearly, the anomalous winds over East Asia in a preceding winter in strong EASM years are significantly different than those in weak EASM years. Northeasterly winds (Fig. 3a) occurred in strong EASM years, and southwesterly winds (Fig. 3a) occurred in weak EASM years. The distributions of anomalous winds indicate that the preceding EAWM is strong during strong EASM years and weak during weak EASM years. Meanwhile, we also calculated the correlation between regionally averaged meridional winds over East Asia (20°–40°N, 100°–130°E) in summer and the surface temperature (Fig. 4a), as well as the meridional 850-hPa winds (Fig. 4b), in the preceding winter. The distributions of correlation coefficients are given in Fig. 4. Obviously negative correlations exceeding the 95% confidence level are located over East Asia, indicating that strong EASM variation is closely linked with the lower surface temperatures and northward meridional winds at 850 hPa over East Asia in the preceding winter and that weak EASM variation is closely linked with the higher surface temperature and southward meridional winds at 850 hPa over East Asia in the preceding winter.

3. Possible mechanisms

3.1 *Influences of EAWM on tropical SST and atmospheric thermal conditions*

Because of the long "memory" of tropical SST provided by oceanic thermal inertia, SST anomalies (SSTAs) play an important role in global climate change, especially by providing and adjusting atmospheric energy. Li and Hu (1987) and Li (1988) noticed that the frequent activities of strong cold air or strong EAWM over East Asia in winter spread energy into the western equatorial Pacific, resulting in weak trade winds near the equator, and further triggering the El Niño–Southern Oscillation (ENSO). Other research has also substantiated the relationship between the winter/summer circulation and SST (Sun and Sun, 1996; Chen et al., 1999; Zhang and Li, 2004; Yang et al., 2005a, b; Zhang and Wang, 2006; Zhou et al., 2007). Figure 5 illustrates the lead–lag correlation between $I_{\rm EAWM}$ (Yan et al., 2009) and SST. The results show that EAWM is closely related to SST variation in the northwest Indo-Pacific region from simultaneous winter (DJF) to autumn (September–October–November, +SON; Figs. 5c–f). Obvious negative correlation exceeding the 95% confidence level in the northwest Indo-Pacific region persists from simultaneous winter (DJF) to lagging autumn (+SON; Figs. 5c–f), but the correlation in preceding summer (−JJA; Fig. 5a) and autumn (−SON; Fig. 5b) before winter is not significant. Lagging correlation distributions indicate that strong EAWMs cause the cold SSTs in the northwest Indo-Pacific region from simultaneous winter to the next autumn.

According to the strong and weak EAWM years defined by Yan et al. (2009), monthly variations of area-averaged SSTAs in the equatorial Indian Ocean (40°–100°E, 10°S–10°N), and the South China Sea (SCS) region (105°–120°E, 10°–25°N) during strong and weak EAWM years are presented in Fig. 6. Tropical SSTs vary differently during strong and weak EAWM years, not only in winter, but also afterward.

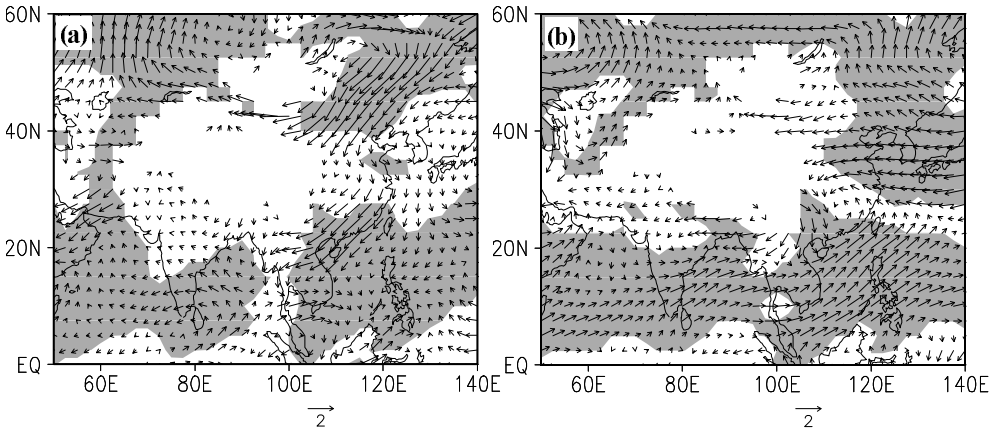

Fig. 3. Composite wind anomalies in preceding winter in (a) strong and (b) weak EASM years. Shading indicates the composite fields exceeding 95% confidence level.

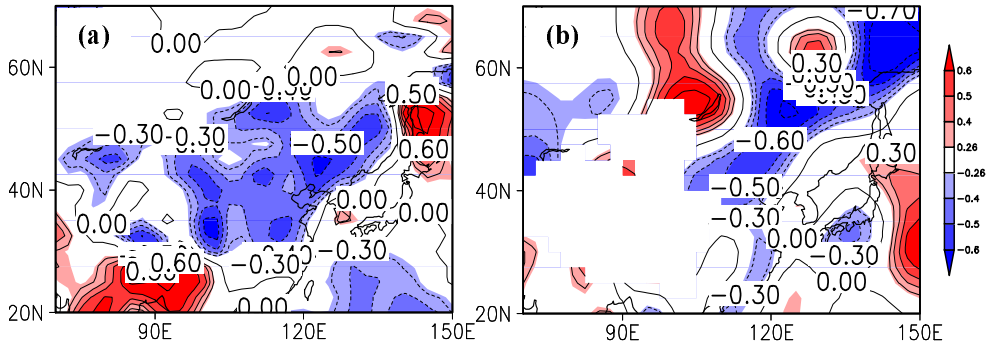

Fig. 4. Correlation between the regionally averaged meridional wind over East Asia (20°–40°N, 100°–130°E) in summer and (a) the surface temperature and (b) the meridional wind at 850 hPa in preceding winter. Shaded areas indicate correlation above the 95% confidence level.

During strong EAWM years, both the equatorial Indian Ocean and the SCS have continuously cold SST anomalies from January to December; but both regions have continuously warm temperature anomalies during weak EAWM years. Sustaining SST variation in the equatorial Indian Ocean is more obvious than that in the SCS region. These persistent SST variations influence the later atmospheric circulation and climate variation through air–sea interactions.

Seasonal variation of the land–sea thermal contrast is an original power of the monsoon formation. Because of obviously different thermal qualities, the SST is higher than the surface temperature over the land in winter, and vice versa in summer, which induces an opposite air stream between land and ocean. Figure 7 exhibits the difference of monthly variation of area-averaged surface temperature (East Asia minus SCS) during strong and weak EAWM years, which to some extent reflects the seasonal variation of the meridional land–sea thermal contrast. The meridional land–sea thermal contrast exhibits evident seasonal variation, but it varies differently between strong and weak EAWM years. The land–sea thermal contrast is negative in winter but positive in summer during strong EAWM years, which is just the opposite during weak EAWM years. According to the seasonal variation of the large-scale, land–sea thermal contrast, temperature is higher over the land than on the sea in summer. Correspondingly, a low-level air stream flows from sea to land. Because of the persistent influence of EAWM anomaly on SST, a secondary land-sea thermal gradient is added to the large-scale, land–sea contrast background, further inducing later EASM anomalies. After strong EAWM years, the anomalous variation of land–sea thermal contrast in summer further strengthens the meridional land–sea thermal contrast (Fig. 7), thereby resulting in the anomaly of the summer atmospheric circulation over East Asia, creating a stronger EASM. After weak EAWM years, the anomalous variation of land–sea thermal contrast in summer further weakens the meridional land–sea thermal contrast (Fig. 7), thereby resulting in the anomaly

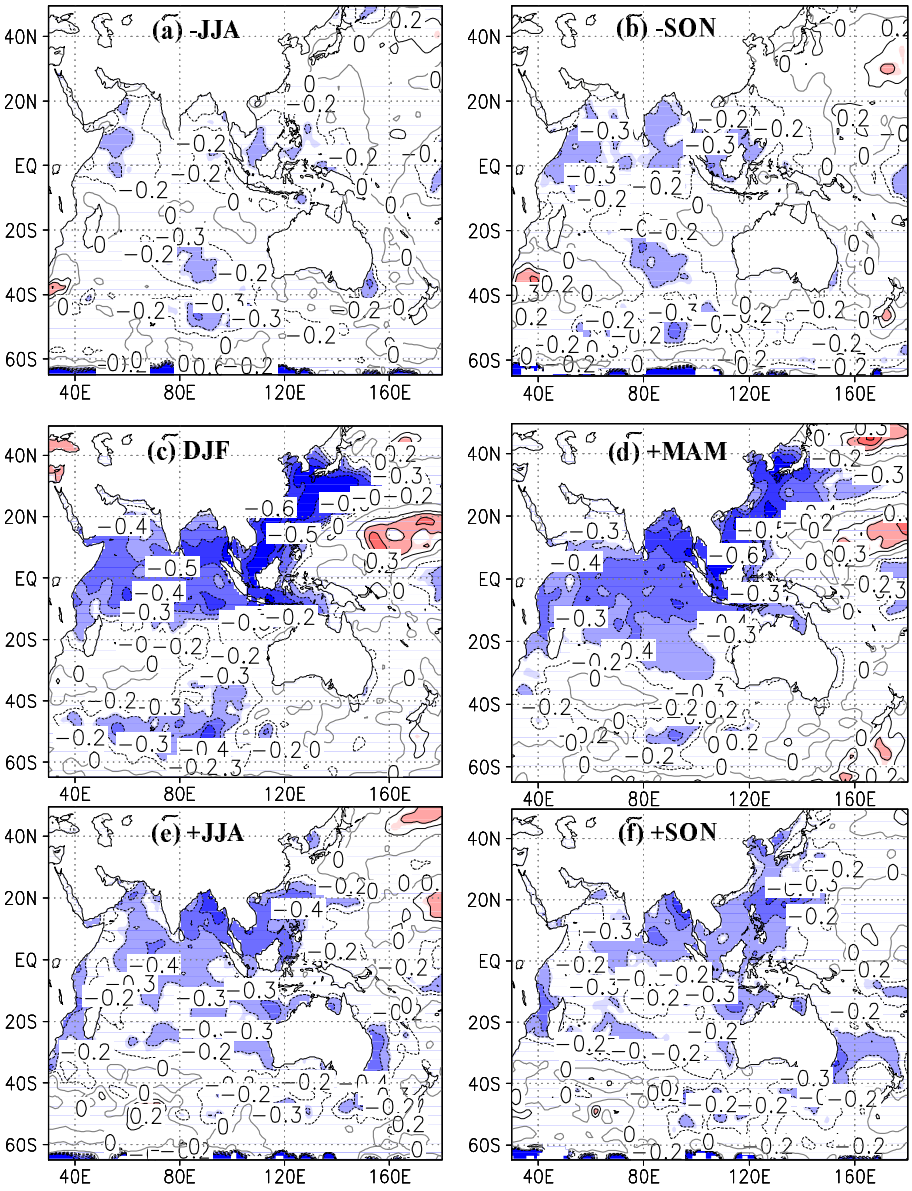

Fig. 5. Correlation between I_{EAWM} and SST (a) preceding summer (−JJA), (b) preceding autumn (−SON), (c) simultaneous winter (DJF), (d) lagging spring (+MAM), (e) lagging summer (+JJA); (f) lagging autumn (+SON).

of the summer atmospheric circulation over East Asia, creating a weaker EASM.

During strong or weak EAWM years, not only does the tropical SST exhibit persistent anomaly, but the low-latitude (10°S–10°N) atmospheric thermal state at lower and upper levels also shows evident discrepancy. The low-latitude troposphere is anomalously cold in the winters of strong EAWM years (Fig. 8a) and is anomalously warm in the winters of weak EAWM years (Fig. 8b). These dynamics maintain cold (strong EAWM years) and warm (weak EAWM years) in the following summer, indicating the duration of the atmospheric thermal state at lower and upper troposphere (Figs. 8c and d). Moreover, the persistent anomaly of the low-latitude atmospheric thermal state from winter to summer has some impact on the variation of the atmospheric thermal contrast over land and sea, and on EASM activities. This subject requires further exploration and is not discussed in this paper.

3.2 *Impacts of persistent SSTA on later atmospheric circulation*

The previous discussion suggests an enduring influence of EAWM on tropical SST and on atmosphere in the lower and upper troposphere. Considering the

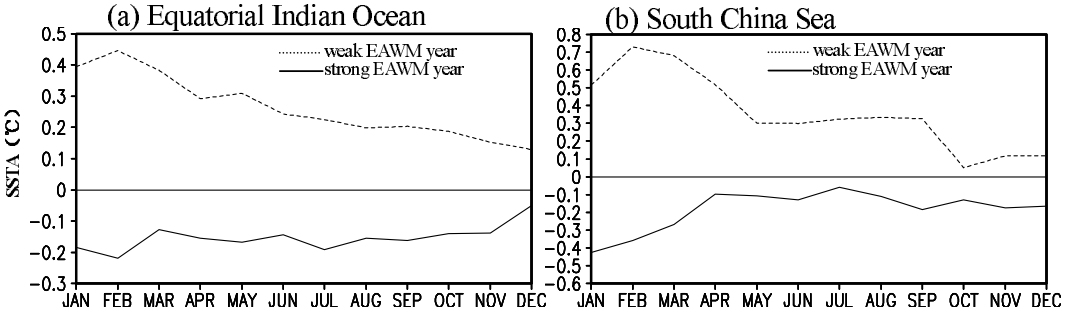

Fig. 6. Monthly variation of SST averaged in (a) the equatorial Indian Ocean (10°S–10°N, 40°–100°E) and (b) South China Sea (10°–25°N, 105°–120°E) during strong (solid line) and weak (dashed line) EAWM years.

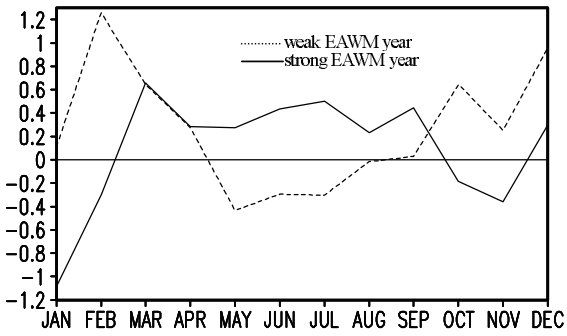

Fig. 7. Monthly meridional thermal contrast in winter between East Asia (30°–40°N, 110°–130°E) and South China Sea (10°–25°N, 105°–120°E) during strong (solid line) and weak (dashed line) EAWM years.

interaction between ocean and atmosphere, how will SST variation impact atmospheric anomalies? Zhou and Wang (2006) reported that variation of the Hadley Cell induced anomalous SST over Indian Ocean and SCS, and that the persistent SST anomalies from spring to summer then consequently resulted in anomalous East Asian summer circulation, further influencing the summer precipitation over the Yangtze River valley. Figure 9 respectively shows the anomalous 850-hPa velocity potential in January and July during strong and weak EAWM years, with negative values indicating anomalous convergence and positive values for anomalous divergence. In the January of strong EAWM years, the anomalous northerly winds over East Asia produce anomalous convergence over the low-latitude regions in Indian Ocean and the western Pacific. In the January of weak EAWM years, the anomalous southerly winds over East Asia produced anomalous divergence over the low-latitude regions in Indian Ocean and the western Pacific. Meanwhile, the anomalous Walker Cell also caused anomalous divergence (Fig. 9a) and convergence (Fig. 9b) over the eastern Pacific. In the following summer, the anomalous velocity potential over the eastern Indo-Pacific region was also significantly different, with the distribution of positive–negative anomalies during strong EAWM years and the distribution of negative–positive anomalies during weak EAWM years (Figs. 9c and d). Positive anomalies over the Indo-Pacific region indicate divergent airflow from the ocean to the East Asian continent, and negative anomalies show convergent airflow from land to ocean.

Variation of the large-scale convergence or divergence over the equatorial Indo-Pacific region in summer directly influences the summer circulation anomaly over East Asia. In the summer after strong EAWM years, the anomalous divergence over the equatorial Indo-Pacific region strengthens the southerly winds in East Asia and therefore results in a stronger EASM. Whereas anomalous convergence weakens the southerly monsoon stream and thus leads to a weaker EASM (Fig. 10). Figure 10 shows that anomalous upward flows are evident near 30°N, therefore causing less summer rainfall over the Yangtze River valley after strong EAWM years and that anomalous downward flows are also evident, causing more summer rainfall after weak EAWM years (Zhao, 1999).

The above analyses indicate that the impacts of EAWM on the tropical SST and persistent SST anomalies possibly play an important role in the relationship between EAWM and EASM, especially in the air–sea interactions over the equatorial Indo-Pacific region. Considering the seasonal shifts in the land–sea thermal contrasts, as well as the variations of the tropical SST and atmospheric circulations during strong or weak EAWM years, reasonable explanations for the interrelation between EAWM and EASM emerge: During strong EAWM year, the persistent cold SSTA over the tropical region strengthens the land–ocean thermal contrast in the following summer, and further strengthens the tropical meridional circulation and the EASM. However, the impacts of the persistent warm

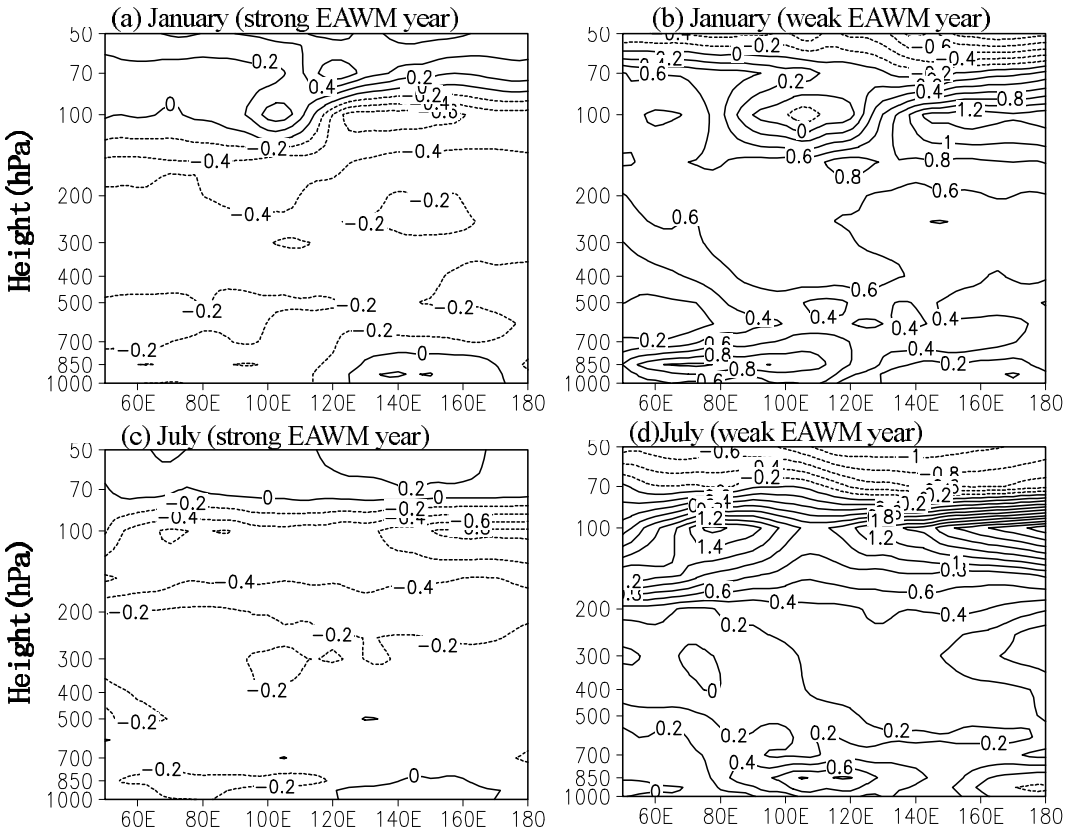

Fig. 8. Longitude-height section of temperature anomalies averaged in 10°S–10°N in (a, b) January and (c, d) July during (a, c) strong and (b, d) weak EAWM years.

SSTs during weak EAWM years cause opposite effect: weakening of the land–ocean thermal contrast in summer, and further weakening of the tropical meridional circulation and EASM. Yan and Xiao (2000) analyzed the influences of the persistent cold and warm Indian Ocean SSTs on EASM activities, concluding that the continuously cold SSTA over the Indian Ocean from winter to summer not only creates an earlier outbreak of EASM but also strengthens the EASM circulation, while the effects of continuously warm SSTAs are the opposite. The results based on data diagnosed in this paper are consistent with their modeling results.

Furthermore, the variation of anomalous velocity potential over the Indo-Pacific region from winter to summer exhibits an evident seasonal variation: convergence or divergence in winter with converse divergence or convergence in summer. The seasonal variation of the airstreams makes stronger EASM following the previous strong EAWM and weaker EASM following the previous weak EAWM. What, then, is the reason for the seasonal variation of the airstreams over the Indo-Pacific region? Apart from the anomalous variation of the land–sea thermal contrast resulting from the persistent tropical SSTAs, seasonal variation of the air streams might also correlate with the seasonal variations of the large-scale mean air stream, and also the SST–radiation–cloud negative feedback. This dynamic process requires more research to be fully understood.

4. Numerical simulation

Previous work (Yan et al., 2009) shows that the variation of the East Asian surface temperature in winter, to a certain extent, reflects the strength of the EAWM, with lower surface temperature during strong EAWM years and higher surface temperature during weak EAWM years. Based on this analysis, this study also further investigated the impacts of EAWM on the EASM by numerical simulation. The global circulation mode (GCM) used in this study was IAP-GCM9L, a nine-level GCM developed from a two-level GCM by the modeling group from the Institute of Atmospheric Physics. The resolution of IAP-GCM is $4^\circ \times 5^\circ$. The model was inspected systematically and strictly using many tests and sensitivity experiments: climatological mean fields for different season, low-frequency oscillation, teleconnection, and others. The model can simulate the basic features of the atmospheric general circulation and its changes, especially Asian monsoon

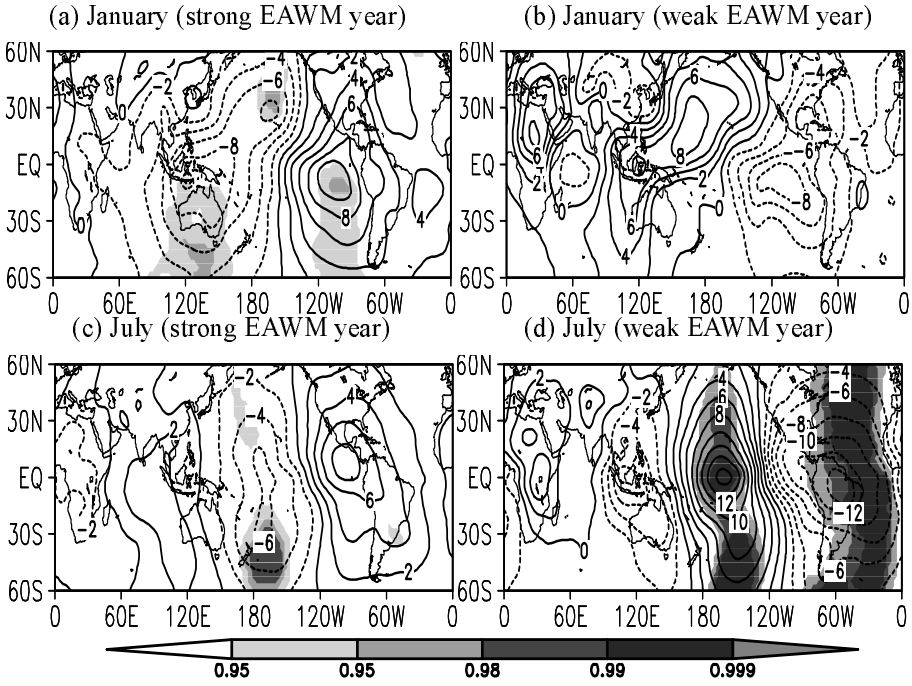

Fig. 9. The 850-hPa stream function in (a, b) January and (c, d) July in (a, c) strong and (b, c) weak EAWM year. Shades indicate the stream function exceeding the 95% confidence level.

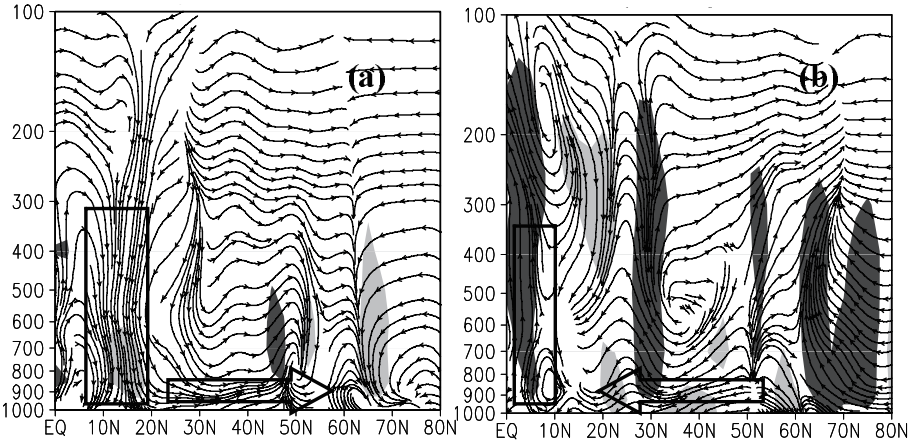

Fig. 10. Longitude-height section of vertical circulation in July averaged in 110°–120°E for (a) strong and (b) weak EAWM year. Shades indicate the vertical velocity above 0.005 m s^{-1}.

activities (Bi, 1993; Liang, 1996).

4.1 *Simulation scheme*

According to the results based on observation data, a numerical simulation scheme is displayed in Fig. 11. Two kinds of anomalous surface temperature gradients were added to the long-time averaged surface-temperature fields. First, anomalous test 1 (Fig. 11a) modeled cold surface temperatures over East Asia (denoted as A1). Second, anomalous test 2 (Fig. 11b) modeled warm surface temperature over East Asia (denoted as A2). Finally, a control test (figure is omitted) modeled the long-time mean surface temperature field (denoted as C). The additional surface temperature anomalies in these two tests to some extent reflect the variation of surface temperature in East Asia during respectively strong and weak EAWM years. The numerical integration time was from January to December, but the anomalous surface temperatures (showed in Fig. 11) were only added for 3 January to 18 Jan-

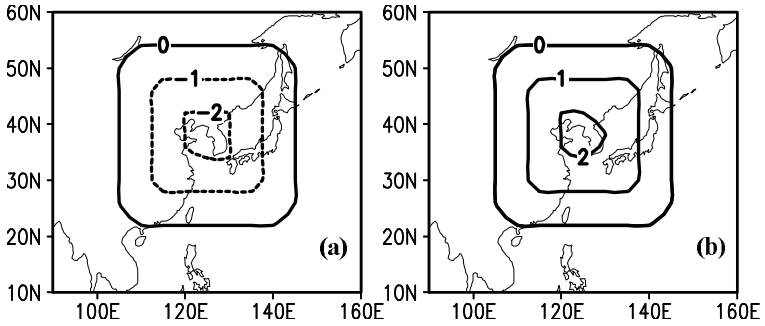

Fig. 11. Simulation scheme of surface temperature in East Asia: (a) cold surface temperature anomalies (A1); (b) warm surface temperature anomalies (A2). Contour interval is 1.0°C.

uary. Considering the influences of different initial fields on the simulation results, we mainly studied the averaged fields of numerical simulation based on five different initial fields. The impact of differing winter warm and cold surface temperatures (i.e., strong and weak EAWMs) on EASMs was analyzed using the output of cold surface temperature test minus that of warm surface temperature test (A1–A2) and the output of the warm surface temperature test minus that of the control test (A2–C). The results of these analyses are presented in the following section.

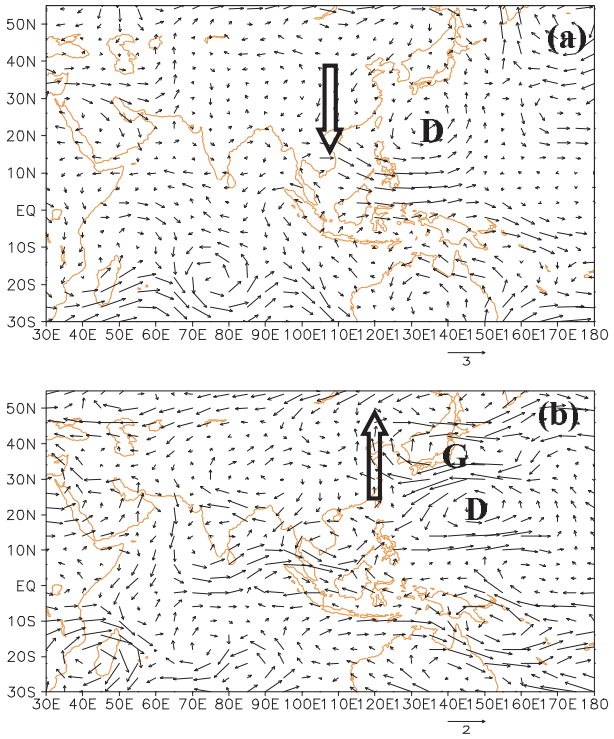

Fig. 12. (a) 850-hPa wind anomaly in JJA of warm surface temperature test minus control test (A2–C). (b) Same as (a), but for the cold surface temperature test minus warm surface temperature test (A1–A2).

4.2 *Numerical simulation results*

Figure 12 shows respectively the low-level 850-hPa wind anomalies in JJA forced by warm surface temperature in winter (Fig. 12a; A2 minus C) and the differences between cold and warm surface temperature test (Fig. 12b, A1 minus A2). In Fig. 12a, an anomalous cyclone was located at the northwestern Pacific region, and anomalous northerlies to the west of the anomalous cyclone controlled the subtropical region in East Asia, indicating that the warm surface temperature in winter made a weak SWPH in the following summer and also a weak EASM. Meanwhile, Fig. 12b shows that an anomalous anticyclone lay in East Asia-northwestern Pacific region at 25°–40°N, with anomalous southerlies in the subtropical region over East Asia, suggesting that cold land surface temperature anomaly in winter results in the SWPH's enhancing and moving northward in the following summer and also correspondingly strengthen the EASM. The influences of EAWM on the following EASM from our numerical simulation were consistent with the results based on observation data of Chen et al. (2000), and our results also support the in-phase variation of EAWM and EASM in the data analyses presented in a previous section herein.

On the other hand, as shown in the anomalous vector wind by modeling, the SWPH was much stronger when it was forced by the cold surface temperatures in January than when it was forced by warm surface temperatures (Fig. 12a).

5. Conclusions

Variations of the atmospheric circulation in different seasons are interrelated and interactive. Based on data analyses and GCMs, this study focused on the relationship between EAWMs and EASMs. Using correlation analyses, composite analyses, and numerical simulations, the interrelationships between EAWMs

and EASMs were investigated based on some representative factors like EAWM index, EASM index, surface temperature and low-level meridional winds over East Asia. Our research results led to the following conclusions:

(1) There is a clear relationship between EAWM and EASM: a strong EAWM favors a stronger EASM in the following summer, whereas a weak EAWM tends to precede a weaker EASM.

(2) Possible mechanisms of the relationship between EAWM and EASM have been determined preliminarily based on the data diagnostics: anomalous EAWMs have a persistent impact on the SST variation over the tropical Indian Ocean and the SCS, and also on the atmospheric thermal anomaly in the lower and upper troposphere in the equatorial region. Through such persistent impact, the anomalous EAWMs affect the land–sea thermal contrast in summer and the atmospheric divergence or convergence over the Indo-Pacific region. Further, they influence the meridional EASM circulation and EASM activities over East Asia. In the summer after a strong EAWM year, divergence over the Indo-Pacific region may enhance the southerly winds in East Asia, leading to a stronger EASM, whereas convergence over the Indo-Pacific region may weaken the southerly winds, resulting in a weaker EASM.

(3) Impacts of the EAWM on the SWPH in summer as exhibited by numerical simulations not only support our data diagnostics but also are consistent with previous research results. This feature illustrates the in-phase variation between EAWM and EASM, and it also provides scientific evidence for the prediction of EASM circulation and climate over East Asia through analysis of preceding EAWM activities and tropical SST variation.

Acknowledgements. The authors acknowledge the support from the National Natural Science Foundation of China (NSFC) under Grant Nos. 40675045 and 41065004, NSFC-Yunnan Joint Foundation under Grant No. U0833602. Comments from two anonymous reviewers were highly appreciated.

REFERENCES

Bi, X. Q., 1993: IAP9L AGCM models and climate numerical simulation. Ph. D. dissertation, Institute of Atmospheric Physics, Chinese Academy of Sciences, 210pp.

Chang, C.-P., and K.-M. Lau, 1982: Short-term planetary-scale interaction over the tropics and the midlatitudes during northern winter, Part I: Contrast between active and inactive periods. *Mon. Wea. Rev.,* **110**, 993–946.

Chen, J., and S. Q. Sun, 1999: Eastern Asian winter monsoon anomaly and variation of global circulation Part I: a comparison study on strong and weak winter monsoon. *Chinese J. Atmos. Sci.*, **23**, 101–111. (in Chinese)

Chen, L. X., Q. G. Zhu, and H. B. Luo, 1991: *East Asian Monsoon*. China Meteorological Press, Beijing, 362pp. (in Chinese).

Chen, W., H. F. Graf, and R. H. Huang, 2000: Interannual variability of East Asian winter monsoon and its relation to the summer monsoon. *Adv. Atmos. Sci.*, **17**, 48–60.

Cui, X. P., and Z. B. Sun, 1999: East Asian winter monsoon index and its variation analysis. *Journal of Nanjing Institute of Meteorology*, **22**, 321–324. (in Chinese)

Ding, Y. H., 1994: *Monsoon over China*. Kluwer Academic Publishers, 419pp.

Gao, H., 2007: Comparison of four East Asian winter monsoon indices. *Acta Meteorological Sinica*, **65**, 272–279. (in Chinese)

Guo, Q. Y., 1983: The summer monsoon intensity index in East Asia and its variation. *Acta Geographica Sinica*, **38**, 207–217. (in Chinese)

Guo, Q. Y., 1985: The variations of East Asian summer monsoon and the rainfall in China. *Tropical Meteorology*, **1**, 44–51. (in Chinese)

Jhun, J. G., and E. J. Lee., 2004: A new East Asian winter monsoon index and associated characteristics of the winter monsoon. *J. Climate*, **15**, 711–726.

Kistler, R., and Coauthors, 2001: The NCEP-NCAR 50-year reanalysis: Monthly means CD-ROM and documentation. *Bull. Amer. Meteor. Soc.*, **82**, 247–268.

Li, C. Y., 1988: Frequent strong East Asia trough activities and the occurrence of the El Niño. *Science in China* (B), **6**, 667–674. (in Chinese)

Li, C. Y., and J. Hu, 1987: Studies on interaction between atmospheric circulation and El Niño. *Scientia Atmospherica Sinica*, **11**, 359–364. (in Chinese)

Li, J. P., and Q. C. Zeng, 2002: A unified monsoon index. *Geophys. Res. Lett.,* **29**(8), 1274, doi: 10.1029/2001GL013874.

Li, J. P., and Q. C. Zeng, 2003: A new monsoon index and the geographical distribution of the global monsoons. *Adv. Atmos. Sci.*, **20**, 299–302.

Li, J. P., and Q. C. Zeng, 2005: A new monsoon index, its interannual variability and relation with monsoon precipitation. *Climatic and Environmental Research*, **10**(3), 351–365. (in Chinese)

Li, Y., and S. Yang, 2010: A dynamical index for the East Asian winter monsoon. *J. Climate*, **23**, 4255–4262.

Liang, X. Z., 1996: Description of a nine-level grid point atmospheric general circulation model. *Adv. Atmos. Sci.*, **13**, 269–298.

Rayner, N. A., D. E. Parker, E. B. Horton, C. K. Folland, L. V. Alexander, D. P. Rowell, E. C. Kent, and A. Kaplan, 2003: Global analyses of SST, sea ice and night marine air temperature since the late nineteenth century. *J. Geophys. Res.*, **108**(D14), 4407, doi: 10.1029/2002JD002670.

Shi, N., 1996: Features of the East Asian winter monsoon intensity on multiple time scale in recent 40 years and their relation to climate. *Journal of Applied meteorological Science*, **7**, 175–181. (in Chinese)

Sun, B. M., and S. Q. Sun, 1996: The role of SST in the East Asian winter monsoon affecting summer drought/flooding in the Yangtze River-Huaihe River valleys. *The Processes of Disastrous Climate and Its Diagnostics*, Huang, Ed., China Meteorological Press, Beijing, 46–53. (in Chinese)

Sun, S. Q., and B. M. Sun, 1995: The relationship between the anomalous winter monsoon circulation over East Asia and summer drought/flooding in the Yangtze and Huaihe River valley. *Acta Meteorologica Sinica*, **53**, 438–450. (in Chinese)

Wang, L., and W. Chen, 2010: How well do existing indices measure the strength of the East Asian winter monsoon? *Adv. Atmos. Sci.*, **27**, 855–870.

Wu, B. Y., and R. H. Huang, 1999: Effects of the Extremes in the North Atlantic Oscillation on East Asia Winter Monsoon. *Scientia Atmospherica Sinica*, **23**, 641–651. (in Chinese)

Yan, H. M., and Z. N. Xiao, 2000: The numerical simulation of the Indian Ocean SSTA influence on climatic variations over Asian monsoon region. *Journal of Tropical Meteorology*, **16**, 18–27. (in Chinese)

Yan, H. M., W. Duan, and Z. N. Xiao, 2003: A study on relation between East Asian winter monsoon and climate change during raining season in China. *Journal of Tropical Meteorology*, **19**, 367–376. (in Chinese)

Yan, H. M., W. Zhou, H. Yang, and Y. Cai, 2009: Definition of a East Asian winter monsoon index and its variation characteristics. *Journal of Nanjing Institute of Meteorology*, **32**, 367–376. (in Chinese)

Yang, H., J. Chen, and S. Q. Sun, 2005a: Numerical experiment on the El Niño event stimulated by the East Asian winter monsoon. *Chinese J. Atmos. Sci.*, **29**, 321–333. (in Chinese)

Yang, H., J. Chen, and S. Q. Sun, 2005b: Numerical experiment on the interseasonal connection of circulation. *Chinese J. Atmos. Sci.*, **29**, 396–408. (in Chinese)

Zhang, Q. Y., and Y. Wang, 2006: The response of East Asian monsoon circulation between winter and summer to sea surface temperature over the Pacific Ocean. *Climatic and Environmental Research*, **11**, 487–498. (in Chinese)

Zhang, R. H., and Q. Li, 2004: Impact of sea temperature variability of tropical oceans on East Asian monsoon. *Meteorological Monthly*, **30**, 22–26. (in Chinese)

Zhang, Y., K. R. Sperber, and J. S. Boyle, 1997: Climatology and interannual variation of the East Asian monsoon: A diagnostic study of the 86/87 and 91/92 events. *J. Meteor. Soc. Japan*, **74**, 49–62.

Zhao, Z. G., 1999: *Summer Drought and Flood of China and Environment Field*. China Meteorological Press, Beijing, 297pp. (in Chinese)

Zhou, B. T., and H. J. Wang, 2006: Relationship between the boreal spring Hadley circulation and the summer precipitation in the Yangtze River valley. *J. Geophys. Res.*, **111**, doi: 10.1029/2005JD007006.

Zhou, W., C. Y. Li, and X. Wang, 2007: Possible connection between Pacific oceanic interdecadal pathway and East Asian winter monsoon. *Geophys. Res. Lett.,* **34**, doi: 10.1029/2006GL027809.